

Electronic Supplementary Information for
**A Tri-layer High-Temperature All-organic Films with Superior
Energy Storage Density and thermal Stability**

Jie Chen^{a,*}, Pansong Wang^a, Zhen Wang^a, Xiaoyong Zhang^a, Weixing Chen^a, and Yifei Wang^{b,*}

^a Shaanxi Key Laboratory of Optoelectronic Functional Materials and Devices, School of Materials Science and Chemical Engineering, Xi'an Technological University, Xi'an 710032, China

^b State Key Laboratory for Mechanical Behavior of Materials, School of Materials Science and Engineering, Xi'an Jiaotong University, Xi'an, 710049, China

* Corresponding authors. chenjie@xatu.edu.cn (J. Chen), yifei.wang@xjtu.edu.cn (Y. Wang)

Supplementary Text

In order to observe the crystallinity and thermal stability of the tri-layered all-organic composites, the heating curve after eliminating the film thermal history is shown in the **Fig. S4**. The glass transition temperature T_g of PC is 197.5°C, which proves that PC has excellent temperature resistance in high temperature environment. Through the tri-layered all-organic structure design of PC layer and PMMA/P(VDF-HFP) blend layer, the T_g of the composite films prepared are all higher than 190°C. The high heat resistance provides a strong guarantee for the application of tri-layered all-organic composites in high temperature environment.

Pure P(VDF-HFP) shows a single melting peak at 167°C, which may be due to

the presence of α phase

$$X_c = \frac{\Delta H_m}{\Delta H_m^* \times 100\%} \quad (\text{S1})$$

The T_m of C-0%-C, C-20%-C and C-40%-C tri-layered all-organic composites are 166°C, 163°C and 157°C respectively. No significant melting peaks were observed for pure PMMA and C-80%-C, because PMMA is an amorphous polymer and excess PMMA addition causes the melting point to disappear. Different phases in P(VDF-HFP) have different melting points, generally α phase slightly higher than β phase. As the content of PMMA increases, the T_m of the tri-layered all-organic composites decreases. On the one hand, it is due to the dilution effect of amorphous PMMA. The crystallinity $X_c(\%)$ of tri-layered all-organic composites is calculated by following equation.

Where in, ΔH_m is the enthalpy of the tri-layered all-organic composites, which can be obtained by integrating the peak area in the DSC curve. ΔH_m^* is the unit mass melting heat value of pure P(VDF-HFP) with 100% crystallinity, which is 104.7 J/g. The crystallinity of C-0%-C, C-20%-C and C-40%-C are 20%, 12.89% and 9.91% respectively, as shown in **Table S1**. This phenomenon can be explained by the dilution effect of the introduced PMMA. C-80%-C has no obvious crystallization peak. The crystallinity and melting point of the tri-layered all-organic composites decrease with the increase of PMMA content, which indicates that P(VDF-HFP) and PMMA polymers have good affinity and miscibility. In fact, the decrease of T_m in different blend composites can be explained by thermodynamic effect, that is, it is effective in the case of crystalline polymer amorphous polymer system, resulting in

the increase of diluent (PMMA) and the decrease of melting point of polymer crystal (P(VDF-HFP)).

According to the energy storage calculation formula, the dielectric constant and dielectric loss are one of the key factors affecting the energy storage density and charge discharge efficiency. Since the charge and dipole polarization and relaxation of polymer dielectric materials depend on time, the dielectric constant and dielectric loss usually change with the change of electric field frequency. The dielectric constant and dielectric loss of the middle blend layer composite and the tri-layered all-organic composite at different frequencies were shown in **Fig. S5**. The dielectric constant and dielectric loss of the middle blends layer composite and tri-layered all-organic composite decrease with the increase of PMMA content. With the increase of PMMA content, the dielectric loss of the middle blend layer composite increases slightly at low frequencies and decreases significantly at high frequencies. The dielectric loss at high frequencies is related to the amorphous relaxation of the polymer chain, which indicates that the introduction of PMMA chain significantly inhibits the migration of P(VDF-HFP) chain during high-frequency polarization, thereby reducing the dielectric loss of the middle blend layer.

Dielectric constant and dielectric loss of P(VDF-HFP), 40% middle blend layer composite, and C-40%-C is shown in **Fig. S6**. Taking the addition of 40% PMMA as an example, the dielectric constant and dielectric loss of 40% middle blend layer composite is lower than that of P(VDF-HFP), linear polymer PMMA has lower molecular polarization capacity and local number of dipoles than ferroelectric

polymer P(VDF-HFP). This will lead to the suppression of the polarization of P(VDF-HFP) in the middle blend layer. Furthermore, the dielectric constant and dielectric loss of the C-40%-C is lower than the corresponding 40% middle blend layer composite because of the low dielectric constant (i.e.~3.18 at 10^7 Hz) and dielectric loss of PC (~0.01 at 10^3 - 10^7 Hz).

According to previous studies, the electric field distribution has an important influence on the breakdown strength of the composites. Under the condition of ensuring the breakdown field strength of each layer, the more uniform the electric field distribution of the inner and outer layers, the more conducive to improving the breakdown strength of the composites. Therefore, the applied electric field on each layer of outer PC and intermediate blends layer of 300 MV/m is calculated respectively. According to the capacitance calculation formula (S2) and the relationship between voltage and electric field:

$$\frac{\varepsilon_0 \varepsilon_C S_C}{d_C} E_C d_C = \frac{\varepsilon_0 \varepsilon_F S_F}{d_F} E_F d_F \quad (S2)$$

Because the outer layer and the intermediate layer in the composite film are continuous structures of equal size, S_C and S_F in formula (S2) are equal. Formula (S2) can be simplified into formula (S3), where subscript h represents the layer with large dielectric constant, and subscript l represents the layer with small dielectric constant.

$$\varepsilon_C E_C = \varepsilon_F E_F \quad (S3)$$

According to Formula (S3), the field strength is inversely proportional to the relative dielectric constant of each layer. A large dielectric constant imposes a small electric field, while a small dielectric constant imposes a large electric field. Similarly,

in the tri-layered structure, when the dielectric constants of the outer layer and the middle layer are different and have a large difference, the electric field applied to the outer layer and the inner layer will be redistributed, and the electric field distribution will be different due to the difference of the polymer medium constants. The electric field exerted by each layer in the composite dielectric film can be calculated in detail with formula (4-4, 4-5).

$$E_F = \frac{U}{d_F + 2 \frac{\varepsilon_F d_C}{\varepsilon_C}} \quad (\text{S4})$$

$$E_C = \frac{U}{2d_C + \frac{\varepsilon_C d_F}{\varepsilon_F}} \quad (\text{S5})$$

In formula (S4,S5), U is the voltage applied to the entire composite dielectric, E_C is the electric field borne by the outer layer, and E_F is the electric field borne by the inner layer. d_C , ε_C is the thickness and dielectric constant of the outer layer, d_F , ε_F is the thickness and dielectric constant of the inner layer, respectively.

According to the ε' and thickness, calculate the electric field applied to the middle layer and outer layer when the applied electric field is 300 MV/m, and the results are shown in the **Fig. S8(a)**. At 10^3 Hz, the dielectric constant of the outer layer is lower than that of the middle layer, and the electric field C-0%-C borne by the PC layer is 464 MV/m. With the increase of PMMA content in the middle layer, the electric field borne by the PC layer gradually decreases, from 409 MV/m of C-20%-C to 377 MV/m of C-40%-C. At the same time, the electric field borne by the middle blend layer gradually increases, from 135 MV/m of C-0%-C to 199 MV/m of C-20%-

C, to 222 MV/m of C-40%-C. The calculation results show that there is a large difference between the electric field of the outer layer and the middle layer in C-0%-C. If the electric field of the outer layer is too high, it is easy to cause breakdown. When the filling ratio of PMMA in the middle layer increases, the electric field borne by different layers becomes more uniform. However, when the PMMA fraction reaches 80%, compared with previous studies, the electric field borne by the interlayer is too high, leading to breakdown degradation. Therefore, introducing PMMA into P(VDF-HFP) can reduce the dielectric difference between the outer layer and the middle layer, and the local electric field between the three layers reaches the most uniform distribution at C-40%-C.

The current density results of the tri-layered all-organic composites are shown in **Fig. S8(b)**. The current density gradually decreases with increasing PMMA content, the leakage current densities of C-0%-C, C-20%-C, C-40%-C, and C-80%-C are 2.83×10^{-7} A/cm², 2.04×10^{-7} A/cm², 1.59×10^{-7} A/cm², and 1.16×10^{-7} A/cm² at 100 MV/m, respectively.

In order to further evaluate the thermal stability of high temperature resistant polymer films at different temperatures, the energy storage density and charge discharge-efficiency of C-0%-C and C-40%-C were compared at 50°C, 100°C, 120°C and 140°C, as shown in **Fig. S11**. P(VDF-HFP) with poor high temperature resistance performance has been successfully applied to high temperature environment through composite high glass transition temperature PC as an outer layer. With the temperature increasing from 50°C to 120°C, the D_{rem} of C-0%-C increases

significantly from $0.31 \mu\text{C}/\text{cm}^2$ to $0.98 \mu\text{C}/\text{cm}^2$ at $300 \text{ MV}/\text{m}$, the increase amplitude is 216.13%, which leads to the deterioration of charge-discharge efficiency from 90.94% to 75.91%, although D_{max} from $6.94 \mu\text{C}/\text{cm}^2$ increased to $7.46 \mu\text{C}/\text{cm}^2$, it is lower than the increase amplitude of D_{rem} , resulting in the electric displacement $D_{\text{max}} - D_{\text{rem}}$ from $6.63 \mu\text{C}/\text{cm}^2$ reduced to $6.49 \mu\text{C}/\text{cm}^2$, which makes the energy storage density gradually decrease with the increase of temperature, from $9.83 \text{ J}/\text{cm}^3$ to $8.93 \text{ J}/\text{cm}^3$, with a decrease of 9.16%.

By introducing 40% PMMA into P(VDF-HFP), the charge-discharge efficiency of C-40%-C at different temperatures has been significantly improved, from C-0%-C 90.94%(@ 50°C), 82.91%(@ 100°C), 75.91%(@ 120°C) to 92.19%(@ 50°C), 87.49%(@ 100°C), 80.9%(@ 120°C) respectively. Thanks to the introduction of PMMA, which has significantly reduced the increase amplitude of D_{rem} , from $0.27 \mu\text{C}/\text{cm}^2$ (@ 50°C) slightly increased to $0.81 \mu\text{C}/\text{cm}^2$ (@ 120°C), the increase amplitude is only 200%, which is 16.13% lower than C-0%-C. Meanwhile, under the premise of not significantly changing D_{max} , the smaller D_{rem} makes C-40%-C obtain a greater $D_{\text{max}} - D_{\text{rem}}$ value ($6.54 \mu\text{C}/\text{cm}^2$ @ $300 \text{ MV}/\text{m}$) than C-0%-C, so that the energy storage density of C-40%-C is higher than that of C-0%-C.

Materials Characteristics

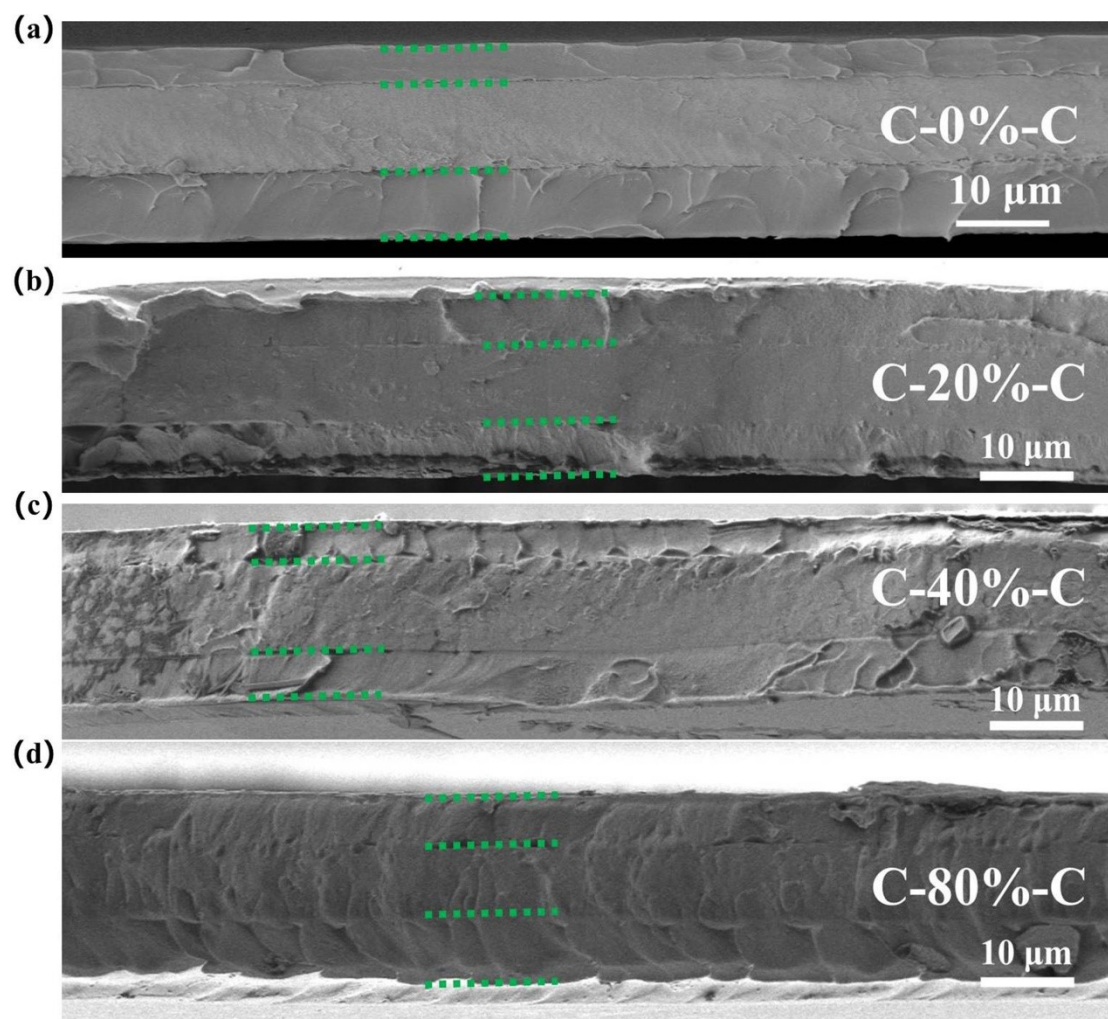


Fig. S1 Cross-sectional SEM images of (a) C-0%-C, (b) C-20%-C, and (c) C-80%-C, respectively.

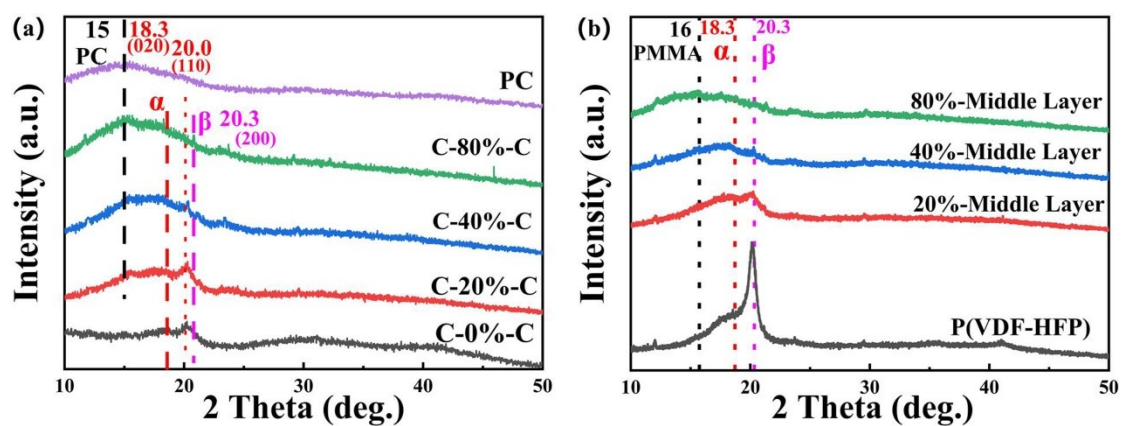


Fig. S2 (a) XRD patterns of tri-layered all-organic composites and PC, (b) XRD patterns of single layered composites and P(VDF-HFP) films, respectively.

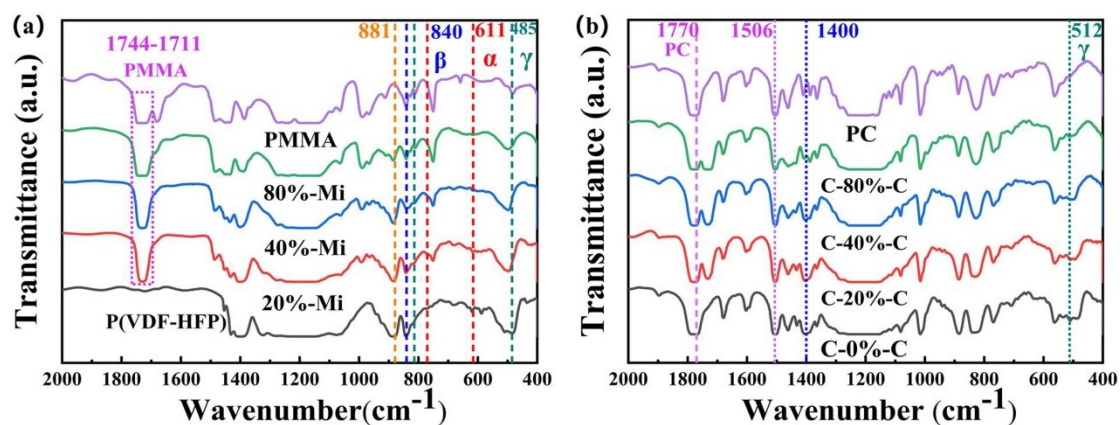


Fig. S3 (a) FTIR patterns of PMMA, P(VDF-HFP), and single layered composites. (b) FTIR patterns of tri-layered all-organic composites and PC.

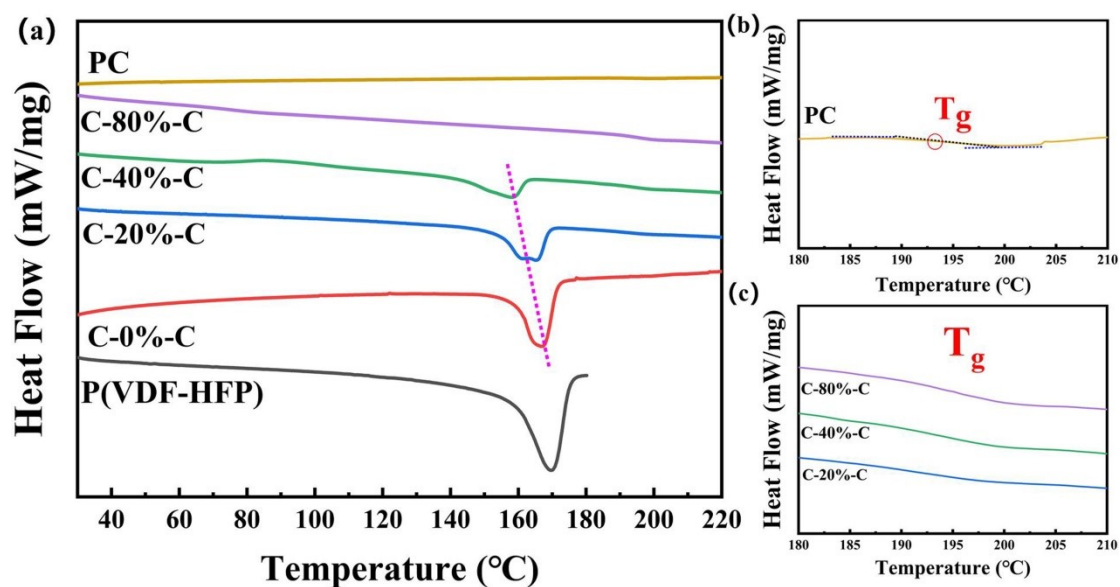


Fig. S4 (a) DSC heating process of PC, PMMA, and tri-layered all-organic composites, respectively, glass transition temperature (T_g) of (b) PC and (c) of tri-layered all-organic composites.

Table S1. The characterization parameters of tri-layered all-organic composites

| PMMA Content | $X_c(\%)$ | $\Delta H_m(\text{J g}^{-1})$ | $T_m^{\text{on}}(\text{°C})$ | $T_m^{\text{off}}(\text{°C})$ | $\Delta T_m(\text{°C})$ | $T_m(\text{°C})$ | $T_g(\text{°C})$ |
|--------------|-----------|-------------------------------|------------------------------|-------------------------------|-------------------------|------------------|------------------|
| 0% | 20 | 20.91 | 150.50°C | 174.51°C | 24.01 | 166.174 | 195.09 |
| 20% | 12.89 | 13.47 | 145.56°C | 171.46°C | 25.9 | 163.23°C | 194.76 |
| 40% | 9.91 | 10.35 | 142.23°C | 163.38°C | 21.15 | 157.93°C | 194.81 |
| 80% | - | - | - | - | - | - | 195.78 |

Dielectric Spectra

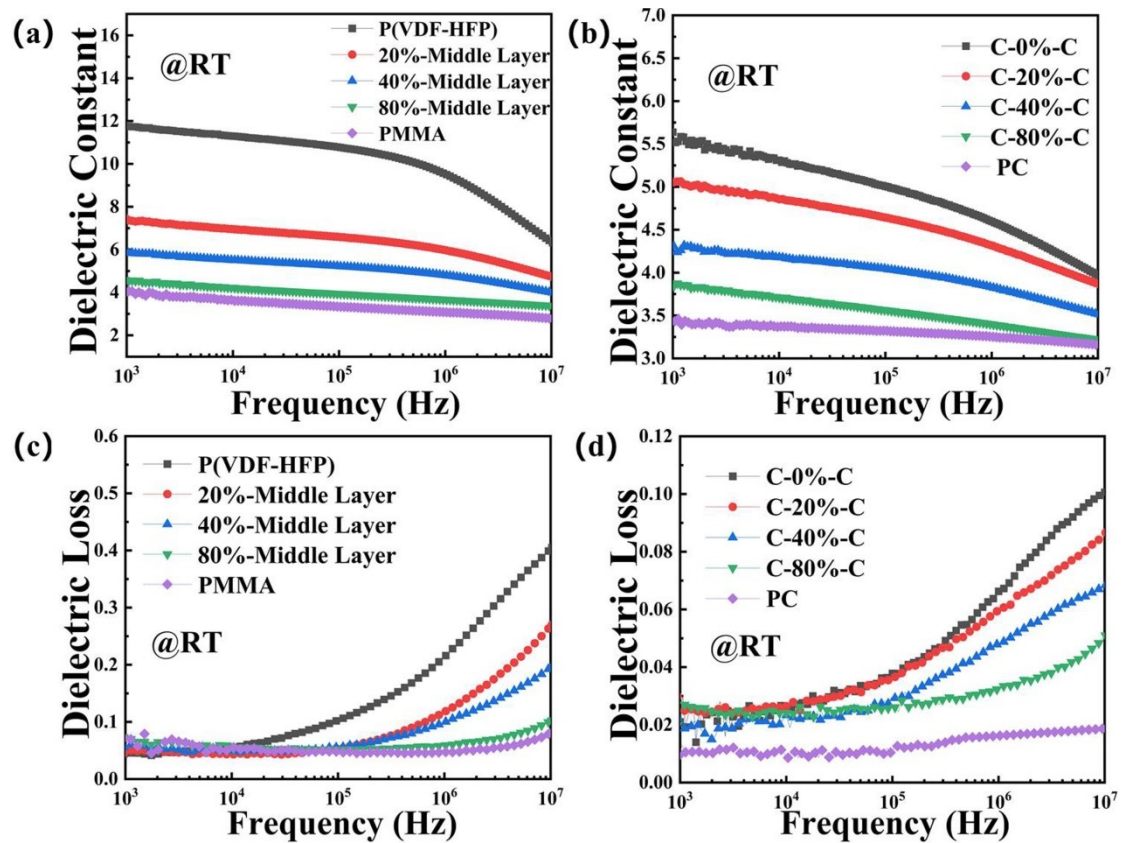


Fig. S5 (a) Dielectric constant and (b) dielectric loss of PMMA, P(VDF-HFP) and single layered composites, respectively, (c) dielectric constant and (d) dielectric loss of PC and tri-layered all-organic composites, respectively.

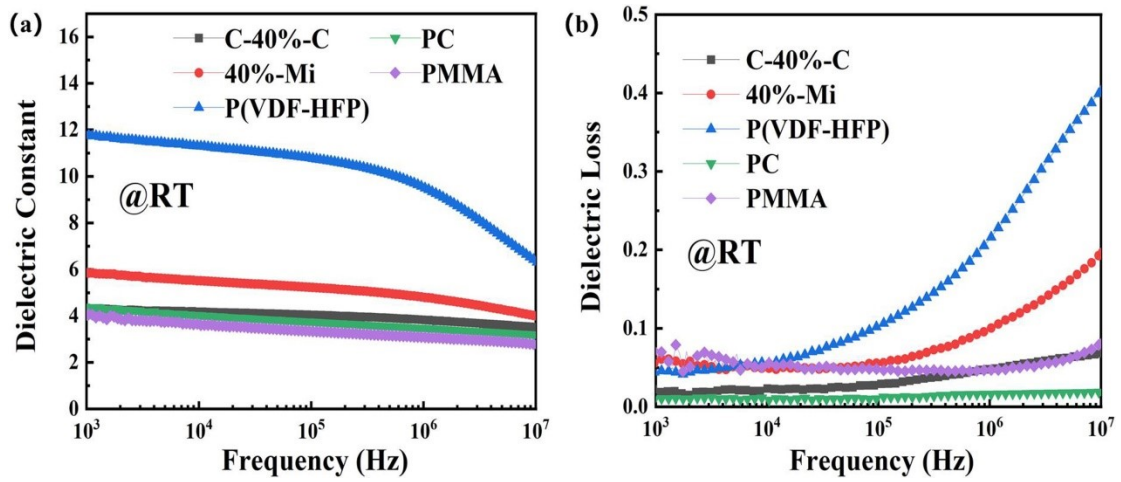


Fig. S6 (a) Dielectric constant and (b) dielectric loss of PC, PMMA, P(VDF-HFP), single layered composite (40%-Mi), and C-40%-C, respectively.

High-Electric-Field Leakage Current Density and Breakdown

Strength

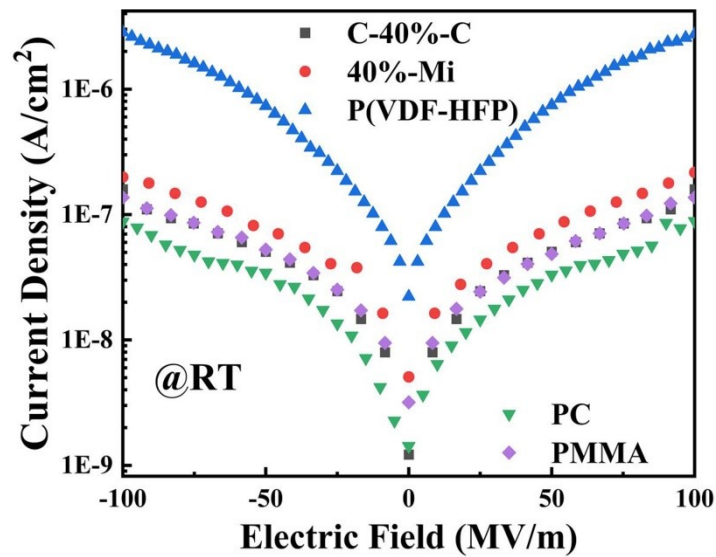


Fig. S7 The leakage current density of PC, PMMA, P(VDF-HFP), single layered composite (40%-Mi), and C-40%-C under different electric fields.

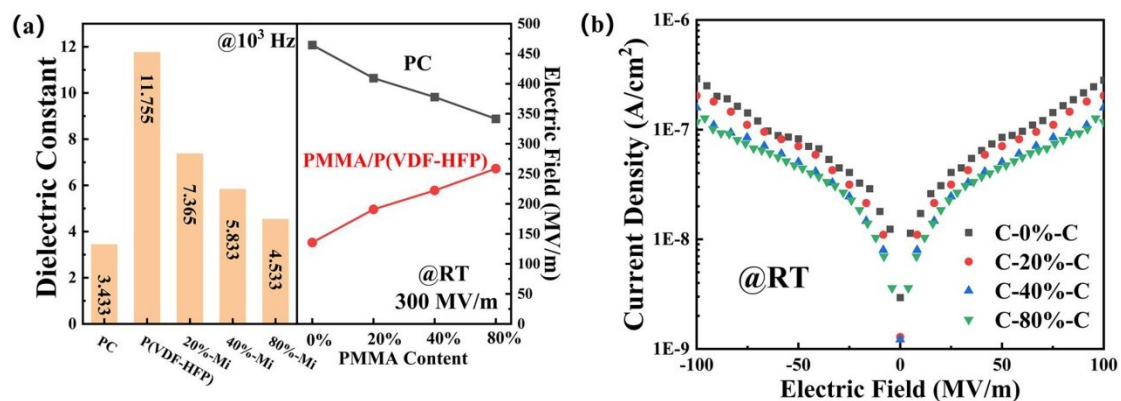


Fig. S8 (a) Dielectric constant and the electric field borne by PMMA/PVDF layer and PC layer for all tri-layered all-organic composites calculated according to the series capacitor model at 300 MV/m. (b) The leakage current density of tri-layered all-organic composites under different electric fields.

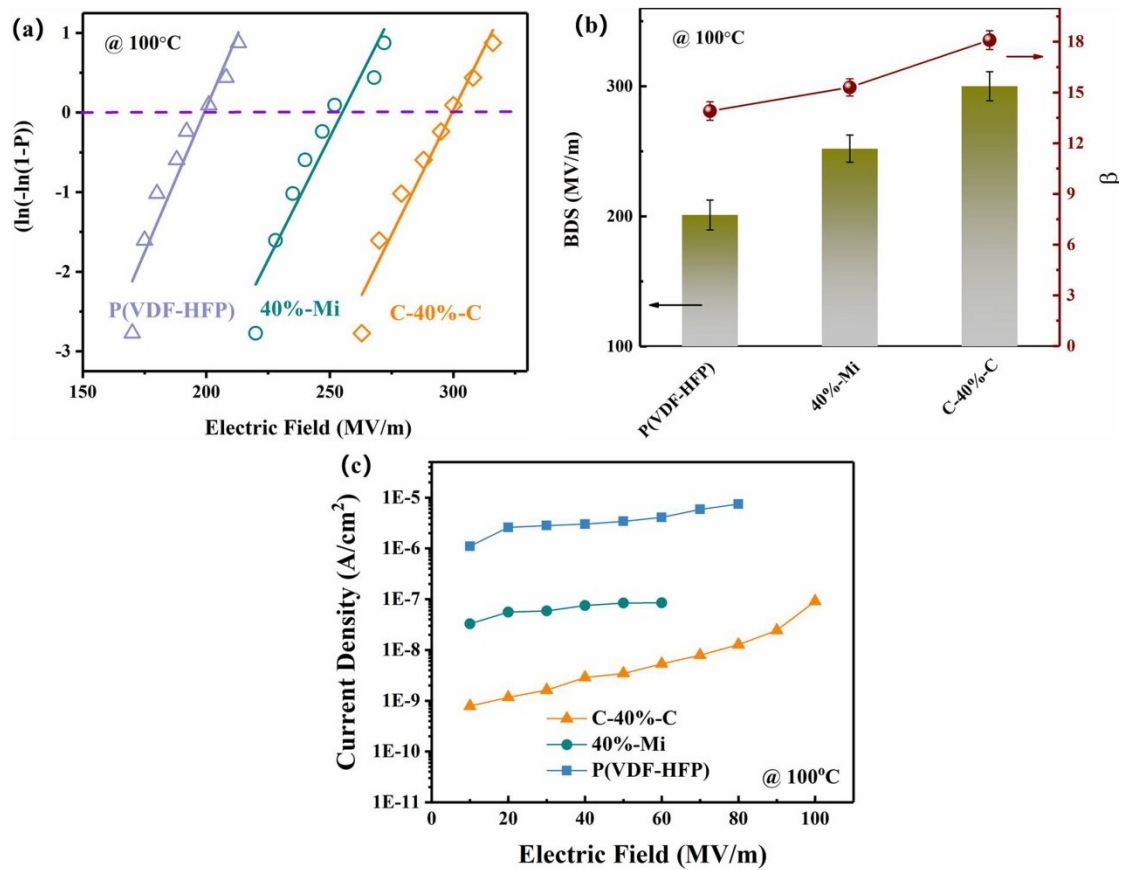


Fig. S9 (a) Weibull distribution of measured breakdown strengths of P(VDF-HFP), single layered composite (40%-Mi), and tri-layered all-organic composite. (b) Breakdown fields and shape parameters for P(VDF-HFP), single layered composite (40%-Mi), and tri-layered all-organic composite. (c) The leakage current density of P(VDF-HFP), single layered composite (40%-Mi), and tri-layered all-organic composite with increasing electric field at 140 °C.

Polarization and Energy Storage

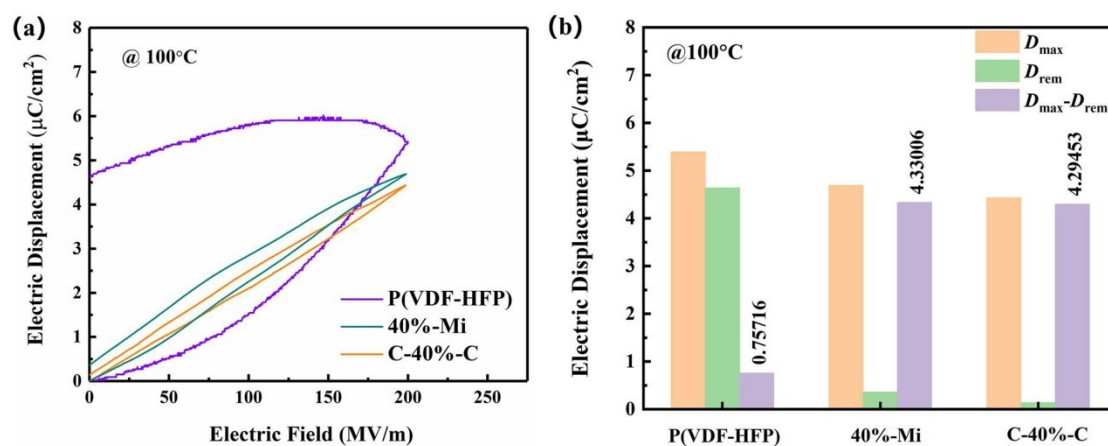


Fig. S10 (a) Unipolar electric displacement-electric field (D - E) loops at 100°C, (b) maximum (D_{max}), remnant displacement (D_{rem}) and electric displacement difference ($D_{\text{max}} - D_{\text{rem}}$) of P(VDF-HFP), single layered composite (40%-Mi), and tri-layered all-organic composite at 200 MV/m.

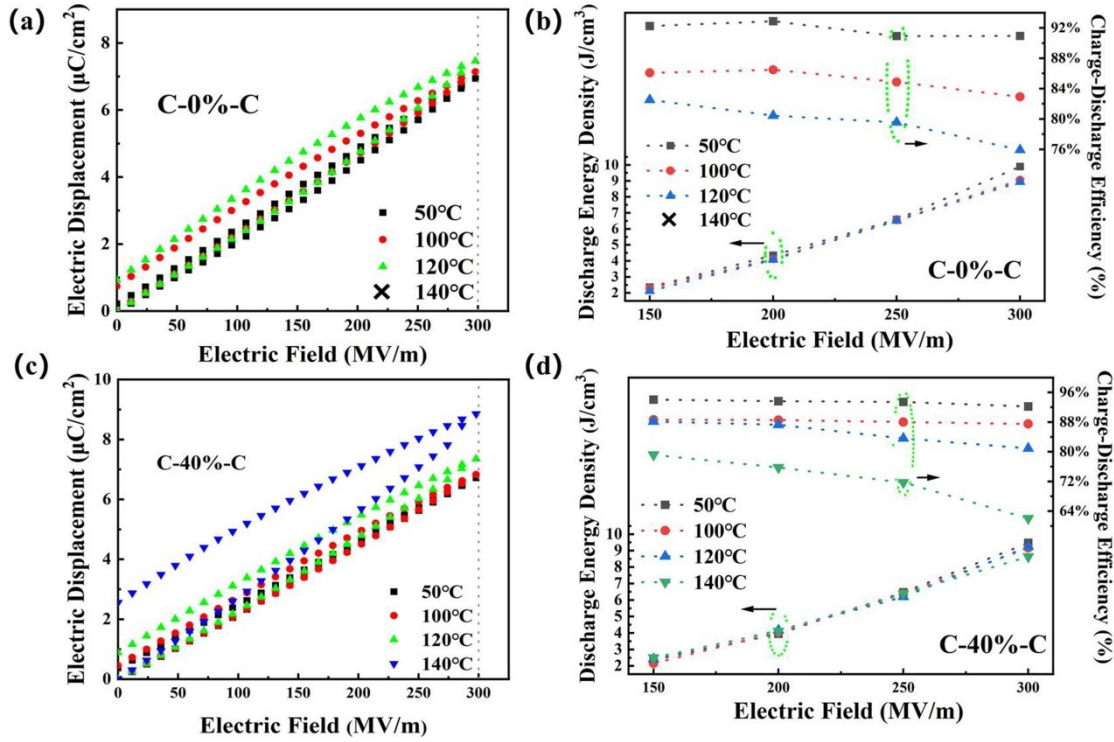


Fig. S11 (a) D - E curves and (b) discharge energy density and charge-discharge efficiency of C-0%-C at 50°C, 100°C and 120°C, (c) D - E curves and (d) discharge energy density and charge-discharge efficiency of C-40%-C at 50°C, 100°C, 120°C, and 140°C.

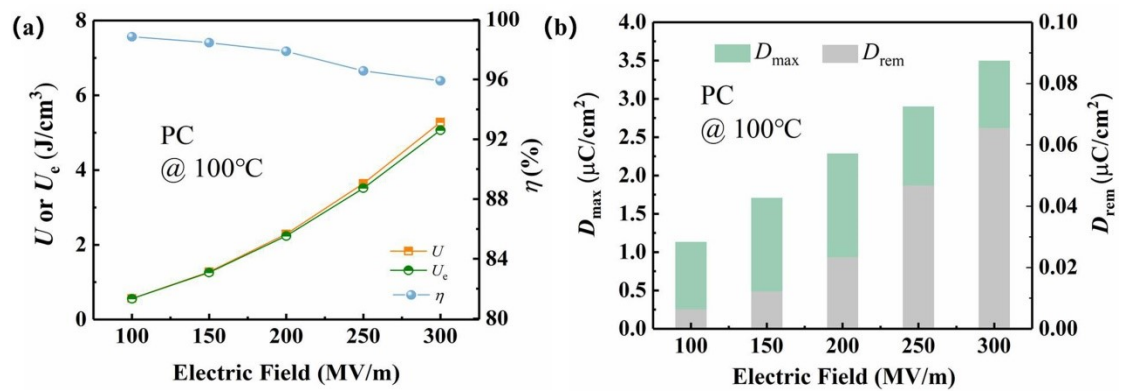


Fig. S12 (a) Charge energy density (U), discharge energy density (U_e), and charge-discharge efficiency (η) of PC at 100 °C and 300 MV/m. (b) D_{\max} and D_{rem} of PC at 100 °C under different electric fields.

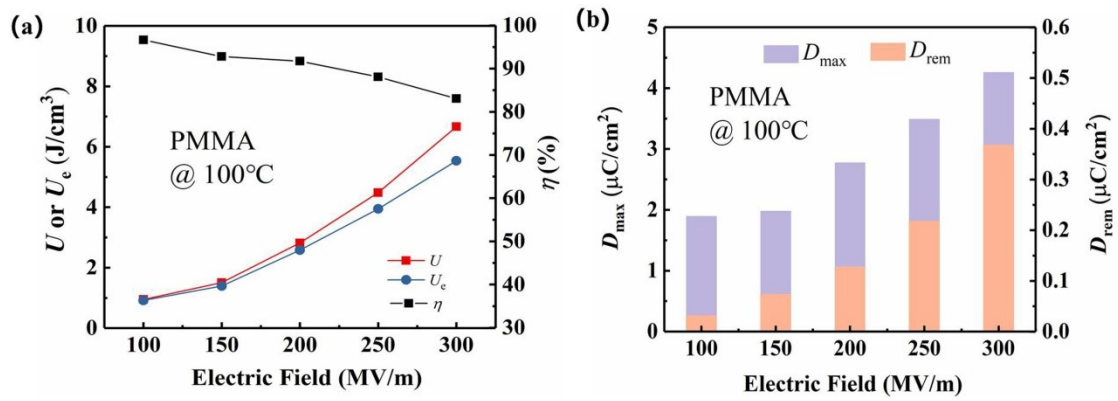


Fig. S13 (a) U , U_e , and η of PMMA at 100 °C and 300 MV/m. (b) D_{max} and D_{rem} of PMMA at 100 °C under different electric fields.

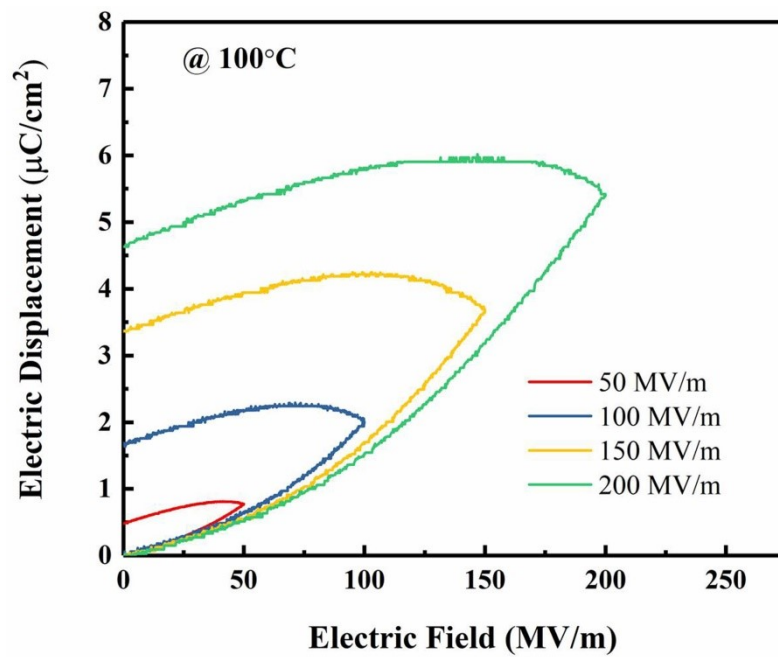


Fig. S14 D - E loops of P(VDF-HFP) at 100°C.